Distinguishing high- from low-temperature platinum nuggets through their trace-element pattern

Alexandre Raphael Cabral[1,2]

Thomas Zack[3,4]

Stephan König[5]

Benjamin Eickmann[5]

Rogerio Kwitko-Ribeiro[6]

Miguel Tupinambá[7]

Bernd Lehmann[8]

[1] Centro de Pesquisas Professor Manoel Teixeira da Costa (CPMTC), Instituto de Geociências, Universidade Federal de Minas Gerais (UFMG), 31270-901, Belo Horizonte-MG, Brazil

[2] Centro de Desenvolvimento da Tecnologia Nuclear (CDTN), 31270-901, Belo Horizonte- MG, Brazil

[3] Department of Earth Sciences, University of Gothenburg, Sweden

[4] Department of Earth Sciences, University of Adelaide, Australia

[5] Isotope Geochemistry, Department of Geosciences, University of Tübingen, Germany

[6] Vale S.A., Departamento de Tecnologia Mineral, 33040-900, Santa Luzia-MG, Brazil

[7] Tektos-Geotectonic Research Group, Faculdade de Geologia, Universidade do Estado do Rio de Janeiro, 20550-050, Rio Janeiro-RJ, Brazil

[8] Mineral Resources, Technische Universität Clausthal, Adolph-Roemer-Str. 2a, 38678 Clausthal-Zellerfeld, Germany

There has been recurrent interest in the origin of platinum nuggets found in alluvial deposits and lateritic covers. Some authors have indicated that platinum nuggets formed from the accessory-mineral spectrum of mantle-sourced melts and, therefore, their occurrence in laterites and placers is detrital in origin ("high-temperature platinum nuggets"; Hattori et al., 1991; Augé and Legendre, 1992; Hattori and Cabri, 1992; Malitch and Thalhammer, 2002; Oberthür et al., 2017). Examples of high-temperature platinum nuggets are known from numerous localities worldwide (Cabri et al., 1996; Weiser, 2002). On the other hand, other researchers have favored that platinum nuggets grew within laterites and placers as a result of dissolution of primary platinum-group minerals, followed by metal precipitation from low-temperature solutions ("low-temperature platinum nuggets"; Cousins and Kinloch, 1976; Bowles, 1986; Aiglsperger et al., 2017; Bowles et al., 2017, 2018). Such a formation has been proposed for some localities, the most spectacular of which are in Minas Gerais, Brazil (Hussak, 1904). However, trace-element compositions of platinum nuggets have scarcely been reported. A trace-element compositional inventory for platinum nuggets of high- and low-temperature origins is thus required to reveal chemical differences that might be used as a fingerprint of the nature of platinum nuggets. Assessing their nature plays an essential role in establishing adequate prospecting criteria for platiniferous mineralization.

In order to distinguish between high- and low-temperature platinum nuggets, we provide reconnaissance in-situ chemical analyses, by means of laser ablation–inductively coupled plasma–mass spectrometry (LA–ICP–MS), of platinum nuggets that have strikingly different morphologies from two historically important placer deposits. High-temperature nuggets come from Chocó, Rio Condoto area, a famous locality in Colombia for coarse nuggets of platinum (von Humboldt, 1826, 1827; Weiser, 2002), representing alluvial Pt–Fe alloys of primary origin from a 20-Ma

Alaskan-type intrusion (Hattori and Cabri, 1992; Tistl et al., 1994; Cabri et al., 1996). The Chocó Pt–Fe nuggets are massive and display worn crystal faces (Fig. 1a, b). Low-temperature nuggets are from Córrego Bom Sucesso, a placer deposit situated in the platiniferous Au–Pd belt of Minas Gerais, Brazil (Cabral et al., 2009). Córrego Bom Sucesso provided the platinum nuggets from which palladium was identified for the first time (Wollaston, 1809; Hussak, 1906; Cassedanne and Alves, 1992). Characteristically botryoidal and arborescent (Fig. 1c, d; Fleet et al., 2002; Cabral et al., 2006), the platinum nuggets from Córrego Bom Sucesso correspond to aggregates formed within the alluvium (Hussak, 1904), likely mediated by microbial activity (Cabral et al., 2011).

Analyses for trace elements were conducted on an Agilent 8800 QQQ ICP–MS system, coupled with an ESI 213 NWR laser ablation system, at the Department of Earth Sciences of the University of Gothenburg. In order to preserve as much precious material as possible for further analyses, nuggets were fixed in the laser ablation chamber only by blue tack. Even though laser spots with a diameter of 50 μm and an energy density of approximately 5.2 J/cm^2 for 60 seconds were focused on unpolished surfaces, stable signals for the entire period allowed straight-forward quantification. As described in König et al (2019), N_2O as a reaction gas in the Agilent 8800 QQQ was used to reduce most unwanted interferences, especially for Se (and Te) quantification. Particularly, the accurate and precise quantification of Se for this study was carefully assessed via comparison of LA–ICP–MS with isotope dilution data following chemical Se purification (Kurzawa et al., 2017; Yierpan et al., 2018; König et al., 2019).

Results of in-situ LA–ICP–MS analyses are presented in Table 1. They demonstrate that the contrasting morphologies of high- and low-temperature platinum nuggets are chemically distinct. All four analyses on two platinum nuggets from Chocó

consistently have higher concentrations of Fe, Ni, Cu, Ru, Rh, Os and Ir than those from Córrego Bom Sucesso. Particularly, Fe and Ir are in the mass-percent range. The results are compatible with the predominance of Pt–Fe alloys and electron-microprobe data that indicate Ir in comparable amounts, as well as the aforementioned elements (Cabri et al., 1996). Our limited dataset is countered by the internal consistency of the results and the representativeness of the nuggets, the morphological and compositional characteristics of which agree with those recorded from Chocó (Cabri et al., 1996; Weiser, 2002).

The platinum nuggets from Córrego Bom Sucesso are depleted in Fe, Ni, Cu and the platinum-group elements, except Pd. Mercury may locally attain concentrations higher than Pt and Pd in the Córrego Bom Sucesso nuggets. These results for Córrego Bom Sucesso agree with previous electron-microprobe data (Fleet et al., 2002; Cabral et al., 2006), as well as in-situ LA–ICP–MS analyses (Cabral et al., 2009). However, the Rh contents reported by Bindi et al. (2013) for the Córrego Bom Sucesso platinum, from 0.10 to 0.30 % (mass), by electron-microprobe analysis, are too elevated compared to ours and may be an artifact of the electron microprobe.

The compositional differences are graphically shown in the multi-element plot of Figure 2. Ruthenium, Rh, Os and Ir are remarkably depleted, up to five orders of magnitude, in the Bom Successo nuggets compared to those from Chocó (Fig. 2a). Iron is also depleted, from three to five orders of magnitude, in the Bom Sucesso nuggets, whereas the Chocó nuggets have S, Fe and Se contents that are similar to the primitive-mantle values (Fig. 2b). Iron forms an alloy with Pt in Chocó nuggets, as indicated by its smooth, plateau-like analytical signal (Fig. 3a), but it occurs in trace amounts as Fe-bearing inclusions within the Bom Sucesso nuggets because of the spiky analytical signal for Fe (Fig. 3b). Contrary to Fe, Se has a plateau-like analytical signal in the Bom Sucesso nuggets, implying the Se is homogeneously incorporated in solid solution (Fig.

3b). In particular, a comparison of S and Se contents in the platinum nuggets discriminates the magmatic versus low-temperature aqueous environment, as shown in a diagram of Se vs. S/Se (Fig. 4). The Chocó and Bom Sucesso nuggets plot apart from each other: the former are above the chondritic S/Se ratio, whereas the latter are undistinguished from Se enrichments found in the weathering zone of seleniferous black shales (Zhu et al., 2014). Such low S/Se ratios in the Bom Sucesso nuggets and in weathered seleniferous black shales imply oxidative recycling of Se and leaching of S in the weathering zone. The large amounts of Se and low S/Se ratios recorded in the platinum nuggets and black shales are unique, and can be explained by Se interaction with organic matter (Cutter, 1982; Zhu et al., 2014), remains of which were found within the Bom Sucesso nuggets (Cabral et al., 2011). Irrespective of whether biological mediation can ultimately originate platinum nuggets (Cabral et al., 2011; Reith et al., 2016), it seems indubitable that supergene recycling of Se in organic-matter-rich milieux is a sine-qua-non condition for Se concentrations exceeding ~100 μg/g Se and S/Se ratios between ~1 and 70. Supergene recycling of Se and its enrichment are compatible with the unusually high concentrations of Pd (Fig. 5), which is the most mobile of the PGE in surficial environments (Wood, 2002).

We conclude that platinum nuggets of supergene origin can effectively be distinguished from residual grains of magmatic origin by means of their fractionated platinum-group-element patterns, their depletion in siderophile and chalcophile elements (Fe, Co, Ni, Cu, Sn), and their diagnostic enrichment in biophile elements such as Se and Hg. The latter can potentially be of practical use as a guide to distinguish between low- and high-temperature platinum nuggets: the latter are poor in Se and Hg (Se <10 μg/g and Hg <100 μg/g); low-temperature platinum nuggets have high contents of Se and Hg (Se >100 μg/g and Hg >1000 μg/g).

This article profited from thoughtful comments by Associate Editor David Holwell and by Larry Meinert's diligent editorial handling. Stephan König acknowledges an ERC Starting Grant (O2RIGIN, 636808).

Appendix 1

Additional elements were analyzed for following the method on-mass vs. mass-shifted mode, as described in Zack and Hogmalm (2016). The elements were: ^{32}S (mass-shifted +32); ^{52}Cr (mass-shifted +16); ^{55}Mn (mass-shifted +16); ^{56}Fe (mass-shifted +16); ^{59}Co (mass-shifted +16); ^{60}Ni (mass-shifted +16); ^{63}Cu (on mass); ^{66}Zn (mass-shifted +16); ^{71}Ga (on mass); ^{72}Ge (mass-shifted +16); ^{75}As (mass-shifted +16); ^{80}Se (mass-shifted +14); ^{95}Mo (on mass); ^{101}Ru (on mass); ^{103}Rh (on mass); ^{105}Pd (on mass); ^{111}Cd (on mass); ^{115}In (on mass); ^{118}Sn (mass-shifted +16); ^{121}Sb (mass-shifted +16); ^{128}Te (mass-shifted +16); ^{185}Re (on mass); ^{189}Os (on mass); ^{193}Ir (on mass); ^{195}Pt (mass-shifted +32); ^{197}Au (on mass); ^{202}Hg (on mass); ^{203}Tl (on mass); ^{208}Pb (on mass); ^{209}Bi (on mass).

In the absence of reference material for platinum nuggets, a combination of several reference materials were used for quantification: for NIST SRM 610, Mass-1, AI-3 and Trans-1 see König et al (2019); for platinum-group-element (PGE) quantification, the sulfide reference material Po-725 was employed (Sylvester et al. 2005). Concentrations of all elements were normalized to 100 per cent (%, mass).

Although several important interferences can be controlled by applying N_2O as a reaction gas – e.g., the elimination of Cu- and Ni-argides on Rh and Pd, respectively, and the reduction of the Sn interference on In –, some interferences specific to PGE nuggets need to be carefully considered. For instance, $^{189}Os^{16}O^+$ would result in a significant overlap on $^{205}Tl^+$, which was mitigated by analyzing ^{203}Tl instead. The influence of $^{193}Ir^{16}O^+$ on $^{209}Bi^+$ signals was corrected by looking at the interference on Ir

alloy (~0.8 ppm apparent Bi for 1 % Ir). Both $^{192}Pt^{16}O^{+}$ and $^{192}Os^{16}O^{+}$ effects on $^{208}Pb^{+}$ measurements make the Pb results unreliable for Córrego Bom Sucesso.

References

Augé, T., and Legendre, O., 1992, Pt–Fe nuggets from alluvial deposits in eastern Madagascar. The Canadian Mineralogist, v. 30, p. 983–1004.

Aiglsperger, T., Proenza, J.A., Font-Bardia, M., Baurier-Aymat, S., Galí, S., Lewis, J.F., and Longo, F., 2017, Supergene neoformation of Pt-Ir-Fe-Ni alloys: multistage grains explain nugget formation in Ni-laterites: Mineralium Deposita, v. 52, p. 1069–1083.

Bindi, L., Zaccarini, F., Garuti, G., and Angeli, N., 2013, The solid solution between platinum and palladium in nature: Mineralogical Magazine, vol. 77, p. 269–274.

Bowles, J.F.W., 1986, The development of platinum-group minerals in laterites: Economic Geology, v. 81, p. 1278–1285.

Bowles, J.F.W., Suárez, S., Prichard, H.M., Fisher, P., 2017, Weathering of PGE sulfides and Pt–Fe alloys in the Freetown Layered Complex, Sierra Leone: Mineralium Deposita, v. 52, p. 1127–1144.

Bowles, J.F.W., Suárez, S., Prichard, H.M., Fisher, P., 2018, The mineralogy, geochemistry and genesis of the alluvial platinum-group minerals of the Freetown Layered Complex, Sierra Leone: Mineralogical Magazine, v. 82(S1), p. S223–S246.

Cabral, A.R., Beaudoin, G., Kwitko, R., Lehmann, B., Polônia, J.C., and Choquette, M., 2006, Platinum-palladium nuggets and mercury-rich palladiferous platinum from Serro, Minas Gerais, Brazil: The Canadian Mineralogist, v. 44, p. 385–397.

Cabral, A.R., Lehmann, B., Tupinambá, M., Schlosser, S., Kwitko-Ribeiro, R., and de Abreu, F.R., 2009, The platiniferous Au–Pd belt of Minas Gerais, Brazil, and genesis of its botryoidal Pt–Pd–Hg aggregates: Economic Geolology, v. 104, p. 1265–1276.

Cabral, A.R., Radtke, M., Munnik, F., Lehmann, B., Reinholz, U., Riesemeier, H., Tupinambá, M., and Kwitko-Ribeiro R., 2011, Iodine in alluvial platinum–palladium nuggets: evidence for biogenic precious-metal fixation. Chemical Geology, v. 281, p. 125–132.

Cabri, L.J., Harris, D.C., and Weiser, T.W., 1996, Mineralogy and distribution of platinum-group mineral (PGM) placer deposits of the world: Exploration and Mining Geology, v. 5, p. 73–167.

Cassedanne, J.P., and Alves, J.N., 1992, Palladium and platinum from Córrego Bom Sucesso, Minas Gerais, Brazil: Mineralogical Record, v. 23, p. 471–474.

Cousins, C.A., and Kinloch, E.D., 1976, Some observations on textures and inclusions in alluvial platinoids: Economic Geology, v. 71, p. 1377–1398.

Cutter, G.A., 1982, Selenium in reducing waters: Science, v. 217, p. 829–831.

Fleet, M.E., de Almeida, C.M., and Angeli, N., 2002, Botryoidal platinum, palladium and potarite from the Bom Sucesso stream, Minas Gerais, Brazil: compositional zoning and origin: The Canadian Mineralogist, v. 40, p. 341–355.

Hattori, K., and Cabri, L.J., 1992, Origin of platinum-group-mineral nuggets inferred from an osmium-isotope study: The Canadian Mineralogist, v. 30, p. 289–301.

Hattori, K., Cabri, L.J., and Hart, S.R., 1991, Osmium isotope ratios of PGM grains associated with the Freetown Layered Complex, Sierra Leone, and their origin: Contributions to Mineralogy and Petrology, v. 109, p.10–18.

Hussak, E., 1904, Über das Vorkommen von Palladium und Platin in Brasilien: Sitzungsberichte der mathematisch-naturwissenschaftlichen Klasse der Kaiserlichen Akademie der Wissenschaften, v. 113, p. 379–466.

Hussak, E., 1906, Über das Vorkommen von Palladium und Platin in Brasilien: Zeitschrift für praktische Geologie, v. 14, p. 284–293.

König, S., Eickmann, B., Zack, T., Yierpan, A., Wille, M., Taubald, H., and Schoenberg, R., 2019, Redox induced sulfur-selenium isotope decoupling recorded in pyrite: Geochimica et Cosmochimica Acta, v. 244, p. 24–39.

Kurzawa, T., König, S., Labidi, J., Yierpan, A., and Schoenberg, R., 2017, A method for Se isotope analysis of low ng-level geological samples via double spike and hydride generation MC-ICP-MS: Chemical Geology, v. 466, p. 219–228.

Malitch, K.N., and Thalhammer, O.A.R., 2002, Pt–Fe nuggets derived from clinopyroxenite–dunite massifs, Russia: a structural, compositional and osmium-isotope study: The Canadian Mineralogist, v. 40, p. 395–418.

McDonough, W.F., and Sun, S.-s., 1995, The composition of the Earth: Chemical Geology, v. 120, p. 223–253.

Oberthür, T., Melcher, F., and Weiser, T.W., 2017, Detrital platinum-group minerals and gold in placers of southeastern Samar Island, Philippines: The Canadian Mineralogist, v. 55, p. 45–62.

Reith, F., Zammit, C.M., Shar, S.S., Etschmann,B., Bottrill, R., Southam, G., Ta, C., Kilburn, M., Oberthür, T., Ball, A.S., and Brugger, J., 2016, Biological role in the transformation of platinum-group mineral grains: Nature Geoscience, v. 9, p. 294–298.

Sylvester, P.J., Cabri, L.J., Tubrett, M.N., McMahon, G., Laflamme, J.H.G., and Peregoedova, A., 2005, Synthesis and evaluation of a fused pyrrhotite standard

reference material for platinum group element and gold analysis by laser ablation-ICP-MS: 10th International Platinum Symposium, Oulu, Geological Survey of Finland, Extend Abstracts, pp. 16–20.

Tistl, M., Burgath, K.P., Höhndorf, A., Kreuzer, H., Muñoz, R., and Salinas, R., 1994, Origin and emplacement of Tertiary ultramafic complexes in northwest Colombia: evidence from geochemistry and K–Ar, Sm–Nd and Rb–Sr isotopes: Earth and Planetary Science Letters, v. 126, p. 41–59.

von Humboldt, A., 1826. Ueber die Lagerung des Platins: Annalen der Physik, v. 83, p. 515–520.

von Humboldt, A., 1827, Größe der Körner von gediegenem Platin: Annalen der Physik, v. 86, p. 487–490.

Weiser, T.W., 2002, Platinum-group minerals (PGM) in placer deposits, in Cabri, L.J., ed., The geology, geochemistry, mineralogy and mineral beneficiation of platinum-group elements: CIM Special Volume 54, p. 721–756.

Wollaston, W.H., 1809, On platina and native palladium from Brazil: Philosophical Transactions, v. 99, p. 189–194.

Wood, S.A., 2002, The aqueous geochemistry of the platinum-group elements with application to ore deposits, in Cabri, L.J., ed., The geology, geochemistry, mineralogy and mineral beneficiation of platinum-group elements: CIM Special Volume 54, p. 211–249.

Yierpan, A., König, S., Labidi, J., Kurzawa, T., Babechuk, M.G., and Schoenberg, R., 2018, Chemical sample processing for combined selenium isotope and selenium–tellurium elemental investigation of the Earth's igneous reservoirs: Geochemistry, Geophysics, Geosystems, doi.org/10.1002/2017GC007299.

Zack, T., and Hogmalm, K.J., 2016, Laser ablation Rb/Sr dating by online chemical separation of Rb and Sr in an oxygen-filled reaction cell: Chemical Geology, v. 437, p. 120–133.

Zhu, J.-M., Johnson, T.M., Clark, S.K., Zhu, X.-K., Wang, X.-L., 2014, Selenium redox cycling during weathering of Se-rich shales: a selenium isotope study: Geochimica et Cosmochimica Acta, v. 126, p. 228–249.

Figure Captions

Fig. 1. Backscattered-electron images of platinum nuggets from Chocó, Colombia (a, b) and Córrego Bom Sucesso, Minas Gerais, Brazil (c, d). The Bom Sucesso nuggets are botryoidal and arborescent, and consists of Pt and Pd in variable amounts. The Chocó nuggets are Pt–Fe intermetallic compounds, mostly isoferroplatinum, exhibiting worn crystal faces.

Fig. 2. Primitive-mantle-normalized concentrations of the platinum-group elements (a) and other metals (b) in platinum nuggets from Chocó and Bom Sucesso. Those from Bom Sucesso are poor in Fe, Cu, Ru, Sn, Os and Ir; concentrations of Co, Ni and As are below the minimum limit of detection. Samples from Chocó are characteristically enriched in Se, Pd and Hg. Primitive-mantle values are from McDonough and Sun (1995). Concentrations of Ru, Rh and Os in the Bom Sucesso nuggets represent the detection limits and are, therefore, maximum values.

Fig. 3. Time-resolved analytical signals of LA–ICP–MS for selected elements in platinum nuggets from Chocó (a) and Bom Sucesso (b). Laser ablation started at ca. 25 s. Iron, Ni, Pd, Os and Ir exhibit plateau-like analytical signals in a, indicating their homogeneous distribution within platinum at the ablation spot. Selenium is close to the background in a, but its signal is remarkably constant in b. Only plateau-like signals were used for quantification; for example, elevated Se signals during the first 10 s of ablation were excluded because of surface contamination.

Fig. 4. Plot of Se vs. S/Se ratios for platinum nuggets from Chocó and Córrego Bom Sucesso. The Chocó nuggets plot close to the chondritic S/Se ratio (McDonough and Sun, 1995), while the Bom Sucesso nuggets are located far below it. The latter are indistinguishable from weathered seleniferous black shales, which acquired extremely high Se contents due to oxidative recycling of Se in the supergene zone (Zhu et al., 2014).

Fig. 5. Diagram of Se vs. Pd for platinum nuggets from Chocó and Córrego Bom Sucesso. The Bom Sucesso nuggets have extremely high Se and Pd contents.

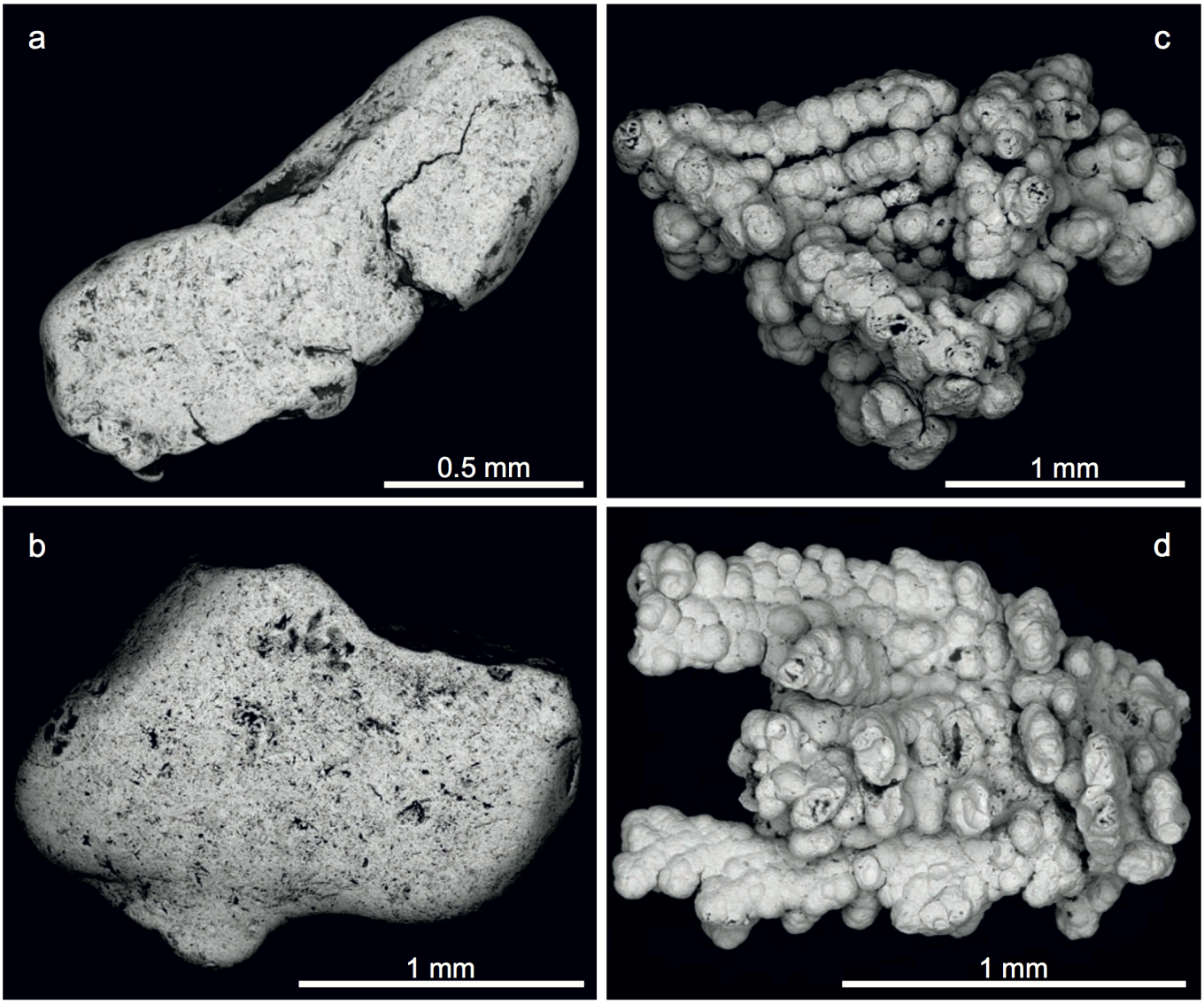

Fig. 1. Backscattered-electron images of platinum nuggets from Chocó, Colombia (a, b) and Córrego Bom Sucesso, Minas Gerais, Brazil (c, d). The Bom Sucesso nuggets are botryoidal and arborescent and consist of Pt and Pd in variable amounts. The Bom Sucesso nuggets are Pt-Fe intermetallic compounds, mostly isoferroplatinum, exhibiting worn crystal faces.

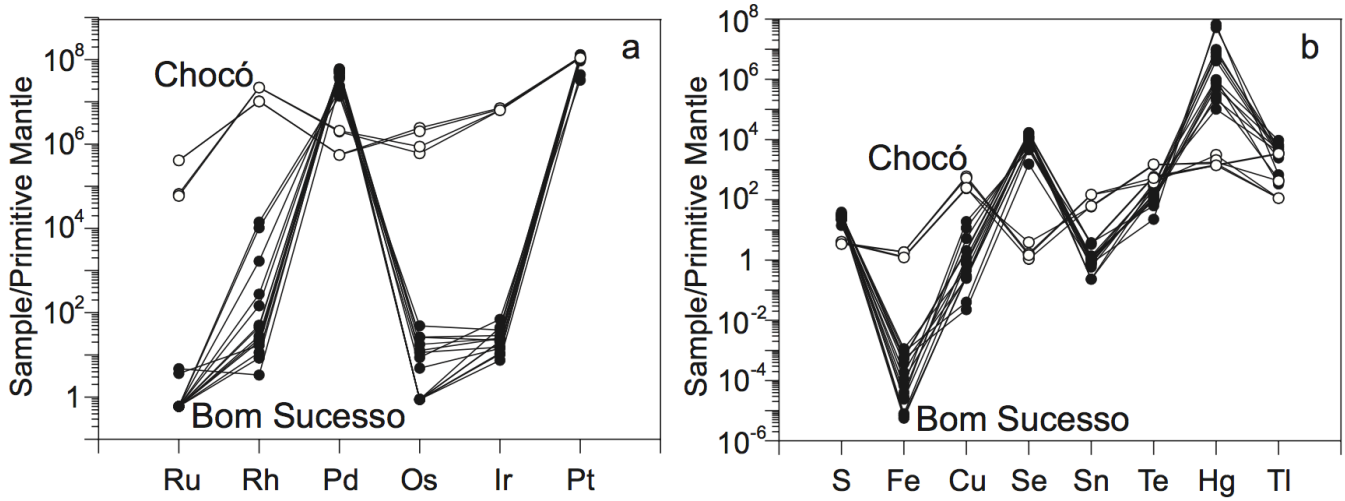

Fig. 2. Primitive mantle-normalized concentrations of the PGE (a) and other metals (b) in platinum nuggets from Chocó and Bom Sucesso. Those from Bom Sucesso are poor in Fe, Cu, Ru, Sn, Os, and Ir; concentrations of Co, Ni, and As are below the minimum limit of detection. Samples from Bom Sucesso are characteristically enriched in Se, Pd, and Hg. Primitive mantle values are from McDonough and Sun (1995). Concentrations of Ru, Rh, and Os in the Bom Sucesso nuggets represent the detection limits and are, therefore, maximum values.

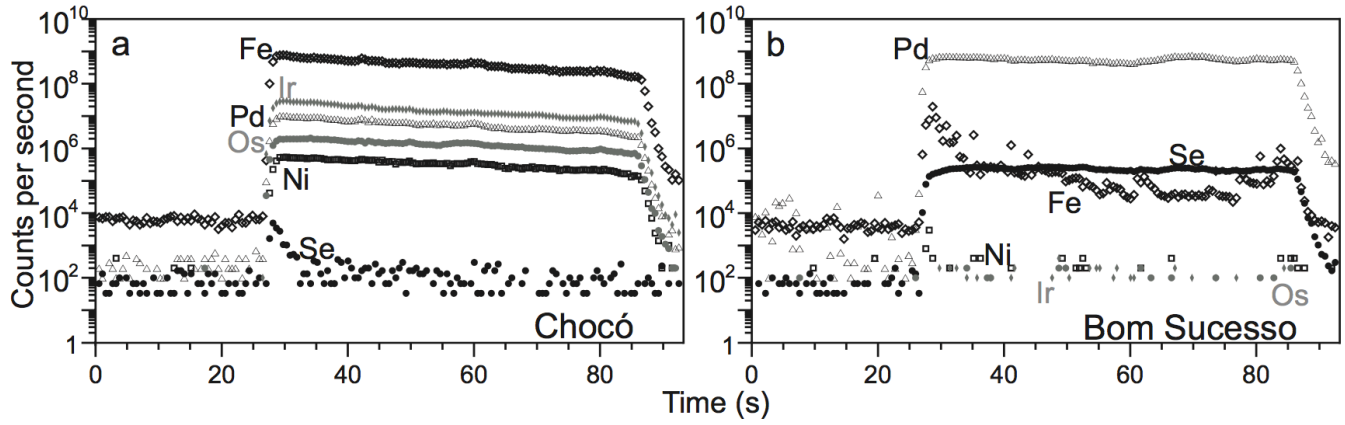

Fig. 3. Time-resolved analytical signals of LA-ICP-MS for selected elements in platinum nuggets from Chocó (a) and Bom Sucesso (b). Laser ablation started at ca. 25 s. Iron, Ni, Pd, Os, and Ir exhibit plateau-like analytical signals in a, indicating their homogeneous distribution within platinum at the ablation spot. Selenium is close to the background in a, but its signal is remarkably constant in b. Only plateau-like signals were used for quantification; for example, elevated Se signals during the first 10 s of ablation were excluded because of surface contamination.

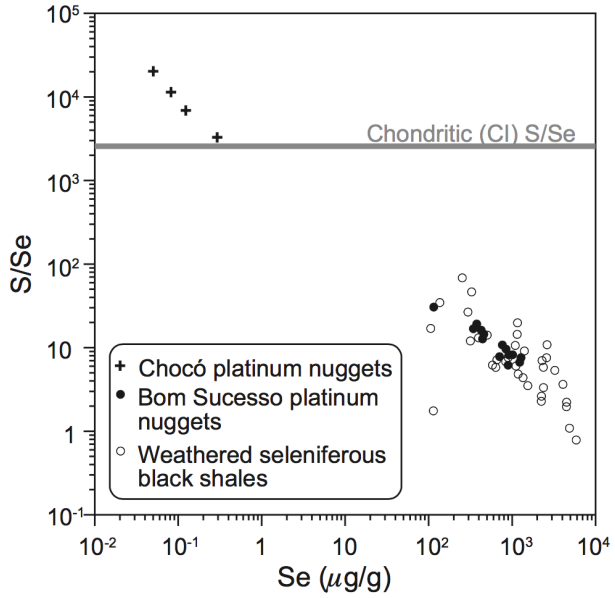

Fig. 4. Plot of Se vs. S/Se ratios for platinum nuggets from Chocó and Córrego Bom Sucesso. The Chocó nuggets plot close to the chondritic S/Se ratio (McDonough and Sun, 1995), while the Bom Sucesso nuggets are located far below it. The latter are indistinguishable from weathered seleniferous black shales, which acquired extremely high Se contents due to oxidative recycling of Se in the supergene zone (Zhu et al., 2014).

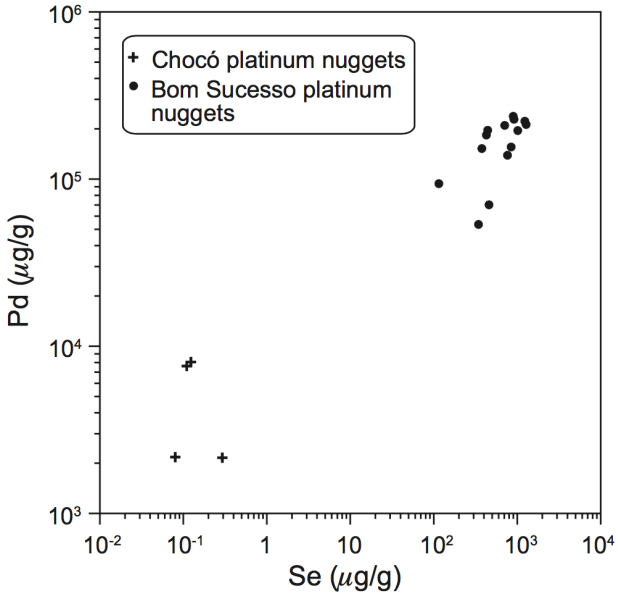

Fig. 5. Diagram of Se vs. Pd for platinum nuggets from Chocó and Córrego Bom Sucesso. The Bom Sucesso nuggets have extremely high Se and Pd contents.

Table 1. Results of LA-ICP-MS Analyses of Platinum Nuggets

		Chocó				Bom Sucesso													
	d.l.	Nugget 1		Nugget 2		Nugget 1		Nugget 2		Nugget 3		Nugget 4		Nugget 5		Nugget 6		Nugget 7	
Spots	μg/g	1	2	3	4	1	2	3	4	5	6	7	8	9	10	11	12	13	14
S	<15	962	1,016	936	848	7,218	3,520	8,238	7,488	8,350	9,692	8,217	8,111	6,656	5,785	6,907	5,617	5,527	5,521
Cr	<0.15	1.77	b.d.l.	b.d.l.	b.d.l.	b.d.l.	b.d.l.	b.d.l.	b.d.l.	b.d.l.	b.d.l.	b.d.l.	b.d.l.	b.d.l.	b.d.l.	b.d.l.	b.d.l.	b.d.l.	b.d.l.
Mn	<0.05	6.3	4.5	3.6	4.8	0.68	0.23	b.d.l.	0.20	b.d.l.	b.d.l.	0.12	0.32	b.d.l.	b.d.l.	0.27	b.d.l.	b.d.l.	b.d.l.
Fe	<0.15	76,471	80,200	117,265	117,362	56	34	37	7.1	1.5	0.50	2.5	71	1.8	4.3	0.43	23	12	0.35
Co	<0.015	54	55	30	32	b.d.l.	b.d.l.	b.d.l.	b.d.l.	b.d.l.	b.d.l.	b.d.l.	b.d.l.	b.d.l.	b.d.l.	b.d.l.	b.d.l.	b.d.l.	b.d.l.
Ni	<0.2	1,394	1,455	352	367	b.d.l.	b.d.l.	b.d.l.	b.d.l.	b.d.l.	b.d.l.	b.d.l.	b.d.l.	b.d.l.	b.d.l.	b.d.l.	b.d.l.	b.d.l.	b.d.l.
Cu	<0.06	7,039	7,533	15,762	17,936	1.2	0.68	62	8.1	36	25	155	14	349	567	7.9	7.4	23	9.0
Zn	<0.4	12	195	17	21	0.6	b.d.l.	b.d.l.	0.7	b.d.l.	b.d.l.	3.2	b.d.l.	b.d.l.	b.d.l.	b.d.l.	b.d.l.	b.d.l.	b.d.l.
Ga	<0.02	0.13	0.05	0.08	0.07	0.06	0.07	0.60	0.05	b.d.l.	b.d.l.	b.d.l.	b.d.l.	b.d.l.	b.d.l.	b.d.l.	b.d.l.	0.06	b.d.l.
Ge	<0.25	b.d.l.	b.d.l.	b.d.l.	b.d.l.	b.d.l.	b.d.l.	b.d.l.	b.d.l.	b.d.l.	b.d.l.	b.d.l.	b.d.l.	b.d.l.	b.d.l.	b.d.l.	b.d.l.	b.d.l.	b.d.l.
As	<0.15	10	11	12	14	b.d.l.	b.d.l.	0.44	b.d.l.	b.d.l.	b.d.l.	b.d.l.	b.d.l.	b.d.l.	b.d.l.	b.d.l.	b.d.l.	0.23	0.20
Se	<0.07	0.29	0.08	0.11	0.12	377	115	1233	914	1015	1,278	764	846	459	344	427	443	707	895
Mo	<0.1	b.d.l.	b.d.l.	b.d.l.	b.d.l.	b.d.l.	b.d.l.	b.d.l.	b.d.l.	b.d.l.	b.d.l.	b.d.l.	b.d.l.	b.d.l.	b.d.l.	b.d.l.	b.d.l.	b.d.l.	b.d.l.
Ru	<0.005	2,041	2,041	294	333	0.022	0.024	b.d.l.	b.d.l.	b.d.l.	b.d.l.	b.d.l.	b.d.l.	b.d.l.	b.d.l.	b.d.l.	b.d.l.	b.d.l.	0.018
Rh	<0.005	9,436	9,183	19,799	19,918	0.021	b.d.l.	0.041	0.008	0.25	0.13	1.51	0.046	12.7	9.3	0.010	0.019	0.025	0.015
Pd	<0.02	2,152	2,172	7,612	8,049	152,289	93,913	221,855	227,891	194,926	212,161	138,820	155,580	70,148	53,525	183,459	195,925	209,370	237,341
Cd	<0.01	0.42	0.16	0.18	0.19	0.34	0.16	0.31	0.52	0.27	0.13	0.10	0.39	0.08	0.10	0.58	0.27	0.26	0.41
In	<0.01	0.05	0.14	0.20	0.17	0.14	0.03	b.d.l.	b.d.l.	b.d.l.	b.d.l.	b.d.l.	b.d.l.	b.d.l.	b.d.l.	b.d.l.	b.d.l.	b.d.l.	b.d.l.
Sn	<0.05	7.5	8.1	19	19	0.49	0.10	0.43	0.14	0.15	b.d.l.	0.08	b.d.l.	0.09	0.15	0.12	0.17	0.18	0.11
Sb	<0.15	4.2	3.7	4.4	5.1	b.d.l.	b.d.l.	b.d.l.	b.d.l.	b.d.l.	b.d.l.	b.d.l.	b.d.l.	b.d.l.	b.d.l.	b.d.l.	b.d.l.	b.d.l.	b.d.l.
Te	<0.1	17	18	4.5	6.3	0.8	0.3	7.1	3.6	1.4	1.6	2.7	3.7	4.4	1.2	1.7	1.1	3.3	1.8
Re	<0.1	b.d.l.	b.d.l.	b.d.l.	b.d.l.	b.d.l.	b.d.l.	b.d.l.	b.d.l.	b.d.l.	b.d.l.	b.d.l.	b.d.l.	b.d.l.	b.d.l.	b.d.l.	b.d.l.	b.d.l.	b.d.l.
Os	<0.005	6,847	8,176	2,057	2,966	b.d.l.	0.030	0.060	b.d.l.	b.d.l.	0.039	0.043	0.089	0.089	0.167	b.d.l.	b.d.l.	0.016	b.d.l.
Ir	<0.005	21,280	22,816	20,172	20,362	0.024	0.223	0.079	0.065	0.143	0.049	0.078	0.093	0.071	0.125	0.033	0.067	0.046	0.035
Pt	<0.07	831,766	825,229	780,134	776,670	313,150	231,194	768,016	664,092	790,328	767,596	849,850	834,262	912,214	936,826	767,842	790,428	726,623	679,688
Au	<0.002	192	192	56	61	92	43	10	1,535	21	52	1.04	1.19	241	34	100	8.0	3.7	3.5
Hg	<0.01	18	16	31	14	522,841	668,059	n.a.	98,016	5,270	9,132	2,122	1,023	9,815	2,822	41,198	7,488	57,490	76,493
Tl	<0.8	1.5	b.d.l.	b.d.l.	b.d.l.	13	2.4	12	13	23	33	17	14	1.2	1.7	11	8.6	13	20
Pb	<1.2	*42*	*3.4*	*29*	*7.9*	*3.3*	*b.d.l.*	*b.d.l.*	*b.d.l.*	*b.d.l.*	*b.d.l.*	*b.d.l.*	*b.d.l.*	*b.d.l.*	*b.d.l.*	*b.d.l.*	*7.3*	*4.8*	*4.6*
Bi	<0.25	6.3	6.4	5.7	5.6	2.3	1.6	5.1	4.6	5.5	4.7	5.7	5.5	6.0	6.4	5.3	6.0	5.2	4.7

Notes: b.d.l.= below detection limit, d.l. = detection limit, n.a. = not analyzed, italics = Pb correction not reliable (see text)